

Chemical size-effects on fluorescence lifetime of Rhodamine 6G in ethylene glycol/water microdroplets dispersed in polydimethylsiloxane matrix

Satoshi Habuchi, Haeng-Boo Kim¹, Noboru Kitamura*

Division of Chemistry, Graduate School of Science, Hokkaido University, Sapporo 060-0810, Japan

Received 6 December 1999; received in revised form 26 January 2000; accepted 8 February 2000

Abstract

The fluorescence dynamics of Rhodamine 6G (R6G) in ethylene glycol/water (EG/W) microdroplets dispersed in a polydimethylsiloxane (PDMS) solid matrix were studied by picosecond time-resolved microspectroscopy. The large decrease in the fluorescence lifetime of R6G was observed for the droplets with the diameter (d) below 10 μm and at the R6G concentrations ($[\text{R6G}]$) above 0.1 mM. Absorption microspectroscopy revealed that the dimer formation of R6G in EG/W microdroplets was facilitated with decreasing d and increasing $[\text{R6G}]$. The size-dependent fluorescence lifetime of R6G was related to quenching of the monomer excited state by the R6G dimer. The origin of size-dependent dimer formation and, thus, the size-dependent fluorescence lifetime of R6G in micrometer-sized droplets in the PDMS matrix was discussed in detail. © 2000 Elsevier Science S.A. All rights reserved.

Keywords: Rhodamine 6G; Polydimethylsiloxane; Ethylene glycol/water

1. Introduction

Chemical characteristics of dye molecules incorporated in single micrometer-sized liquid droplets can be now studied directly by using a microspectroscopy technique combined with an optical- or electrodynamic-trapping method for individual droplets [1]. Recent reports demonstrate that the refractive index relation between a microdroplet (n_d) and the surrounding medium (n_m) is one of the important factors deciding the optical and excited-state behaviors of a dye in microdroplets. At $n_d > n_m$, it has been reported that dye emission from a droplet interior is reflected at the droplet/medium interface through a total-internal reflection phenomenon and, thus, the microdroplet can act as a spherical cavity [2]. On the basis of such an effect, lasing emission [3–8], a modified-spontaneous emission rate of a dye, [9–11] and enhanced energy transfer [12,13] can be observed in microdroplets. Since the optical cavity effect is related to the size of a droplet, both spectroscopic and dynamic properties of dye emission is dependent on the size of a microdroplet. In practice, Barnes et al. reported that the fluorescence lifetime of Rhodamine 6G (R6G) in an ethylene glycol (EG) microdroplet levitated in air (i.e., $n_d > n_m$) decreased with a

decrease in the droplet diameter (d ; $d < 8 \mu\text{m}$) through a cavity-enhanced spontaneous emission rate [14]. In the case of EG microdroplets in a silicon oil, Pandey and Hirayama also reported that the fluorescence lifetime of R6G was shorter for smaller-sized droplets: $d < 10 \mu\text{m}$ [15]. They attributed this size-dependent fluorescence lifetime to enhanced energy transfer between the R6G molecules in the microdroplet with some contributions from the optical cavity effects.

On the other hand, it has been demonstrated that chemical reactions and processes in a microdroplet or across a microdroplet/solution interface are also dependent on d . As an example, our group reported previously that molecular association of a dye molecule in individual water droplets dispersed in dioctylphthalate or dibutylphthalate was facilitated by decreasing the droplet size [16,17]. The rates of electron transfer and mass transfer across single microdroplet/water interfaces have been also shown to depend on d [18–20]. Since a decrease in a droplet size renders an increase in the droplet surface area/volume ratio, the role of the surface or interface becomes important for smaller-sized droplets. Therefore, various phenomena in a droplet or across a droplet/solution interface should depend on the droplet size through both physical and chemical effects. In order to understand characteristic phenomena in micrometer dimensions, further detailed investigations are absolutely necessary.

* Corresponding author.

¹ Co-corresponding author.

In this report, we demonstrate chemical size-effects on the fluorescence lifetime of R6G in microdroplets dispersed in a polymer matrix. So far, spectroscopic and excited state properties of dye molecules in individual droplets have been discussed based on dynamic fluorescence spectroscopy in special reference to a d dependence of the fluorescence lifetime. However, the droplet size effects are governed by many factors as mentioned earlier, so that complementary studies of the same system by available spectroscopies are desired. In the present study, therefore, we applied both absorption [18,21–24] and confocal dynamic fluorescence microspectroscopies [25,26]. As a dye molecule, we used R6G, since droplet size effects have been studied widely by using R6G and the results were discussed in terms of the optical cavity effects. By the analogous reason, we employed an ethylene glycol/water (EG/W) mixture as drops. On the other hand, manipulation of individual microdroplets has been conducted in air or solution by an electrodynamic trap [27] or optical trapping technique [18], respectively. However, solvent evaporation cannot be avoided for droplets in air [28]. Furthermore, an application of confocal fluorescence microspectroscopy is in general difficult for levitated droplets. Another possible approach to study individual microdroplets is fixation of microdroplets in a solid matrix. Therefore, we chose optically transparent (in the visible region) polydimethylsiloxane (PDMS) as a solid matrix. Although commercially available, PDMS is a viscous liquid at room temperature, it solidifies upon heating to 65°C, so that R6G–EG/W microdroplets can be easily dispersed and fixed in a PDMS solid matrix. Using R6G–EG/W microdroplets in PDMS as a sample, we report droplet size effects on the fluorescence lifetime of R6G, and the size effects are discussed in terms of the size-dependent dimer formation of R6G.

2. Experimental

2.1. Chemicals and sample preparation

Water was purified by distillation and deionization prior to use (GSR-200, Advantec Toyo Co., Ltd.). Rhodamine 6G (R6G, Tokyo Kasei; Ace grade) and ethylene glycol (EG, Wako Pure Chemical Industries, Ltd.) were used as supplied. The purity of R6G was checked by comparing the molar absorptivity at a maximum wavelength with the reported value [29] and also by the fluorescence lifetime in a dilute aqueous solution [30]. Polydimethylsiloxane (PDMS, Dow Corning) was used as received.

In the present study, the following procedures were employed to prepare ethylene glycol/water (EG/W=1/1 wt.%) microdroplets in a PDMS solid film. PDMS was mixed with a hardening agent just before sample preparation (hardening agent/PDMS=1/10 wt.%). An R6G ([R6G]=5, 2.5, 1, 0.1, 0.01×10^{-3} M) EG/W solution of 40 μ l was injected into the PDMS solution (2 g), and the mixture was stirred by a mechanical stirrer for 1 min at room temperature. The resultant mixture was spread onto a slide glass, and heated at 65°C for 10 min to solidify PDMS: thickness of the film ~ 100 μ m. EG/W microdroplets with d of 1–50 μ m were obtained by these procedures.

2.2. Spectroscopic measurements

Fluorescence decay profiles of R6G in single microdroplets were obtained by a system reported earlier [31] with some modifications by using a confocal fluorescence microscope (Fig. 1). Excitation laser pulses (Coherent, 500 nm, FWHM=150 fs, repetition rate=100 kHz, s-polarized) were

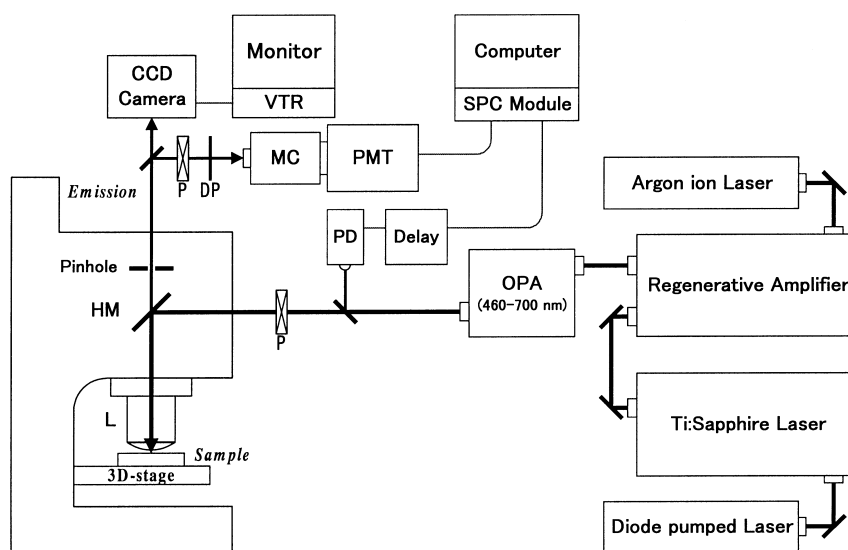


Fig. 1. Block diagram of a confocal fluorescence microspectroscopy system: OPA; optical parametric amplifier, P; polarizer, DP; depolarizer, MC; monochromator, PMT; photomultiplier, PD; pin photodiode, HM; half-mirror, L; oil-immersion objective lens.

introduced to a confocal fluorescence microscope (Olympus, BX-50) and irradiated onto a single microdroplet (spot size $\sim 1 \mu\text{m}$) through an objective lens ($\times 100$ oil, N.A.=1.35). Incident laser power was kept as low as possible to avoid photodegradation of R6G. The R6G emission from an individual microdroplet was collected by the same objective and imaged onto a pinhole set in front of a polychromator. The diameter of the pinhole was selected in between 0.1 and 2 mm to attain spatial resolution (along the laser beam (z) axis) of the spectroscopy in 1–20 μm . Under such conditions, we observed the fluorescence from a whole or part of a microdroplet with minimum background-noises caused by other droplets. The fluorescence being passed through the pinhole was analyzed by a time-correlated single photon counting module (Edinburgh Instruments, SPC-300), equipped with a microchannel plate photomultiplier (Hamamatsu Photonics, R3809U-50) and a polychromator (Jobin Yvon, H-20). A polarizer was set in front of the detector system at a magic angle (49.6°) to cancel fluorescence polarization effects on decay profiles². The monitoring wavelength of the fluorescence was set at 560 nm throughout the study. Decay profiles were analyzed by using an iterative nonlinear least-squares deconvolution method.

Absorption spectra of R6G in individual microdroplets were measured by a microspectroscopy system reported earlier [22–25,32]. The incident light intensity was determined by passing the probe beam (Xe lamp) through a PDMS film without a microdroplet or a dye-free droplet whose size was identical to that of the sample. All the experiments were performed under aerated conditions in a temperature-controlled room (294 K).

3. Results and discussion

3.1. Droplet-size dependence of the R6G fluorescence lifetime

Fig. 2 shows a typical example of the fluorescence decay curves of R6G ($[\text{R6G}]=5 \times 10^{-3} \text{ M}$) in individual microdroplets with different diameters (d). For the droplets with $d > 20 \mu\text{m}$, the fluorescence decay curves were coincident with that in a bulk solution. When d was smaller than $20 \mu\text{m}$, on the other hand, the fluorescence decay was faster for smaller-sized droplets: ‘micrometer size-effects’. A fluorescence decay of R6G at a high concentration has often been analyzed by a model which considers excitation energy migration between the monomers and subsequent energy trap by dimer sites [33–36]. In such a case, the fluorescence shows a non-single exponential decay. In the present

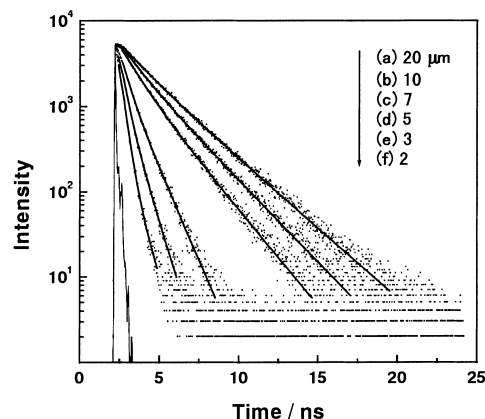


Fig. 2. Fluorescence decay profiles of R6G ($[\text{R6G}]=5 \times 10^{-3} \text{ M}$) in single EG/W microdroplets. Droplet diameters are (a) 20; (b) 10; (c) 7; (d) 5; (e) 3; and (f) 2 μm . The solid curve shows the best fits by double exponential functions.

case at $[\text{R6G}]=5 \times 10^{-3} \text{ M}$, a deviation of the decay profile from a single exponential function became pronounced with a decrease in d , and the decay profile was best analyzed by a double exponential function; as a typical example ($d=5 \mu\text{m}$), the time constants were 1.0 and 0.45 ns.

In the followings, we discuss the present results on the basis of the average fluorescence lifetime ($\langle\tau\rangle$) of R6G in single droplets,

$$\langle\tau\rangle = \frac{\sum_i a_i \tau_i^2}{\sum_i a_i \tau_i} \quad (1)$$

where τ_i and a_i are the fluorescence lifetime and pre-exponential factor of the i th decay component ($i=1, 2$), respectively. The droplet size effects on the average lifetime are shown in Fig. 3, in which the data obtained at other R6G concentrations ($[\text{R6G}]=2.5, 1, 0.1$, or $0.01 \times 10^{-3} \text{ M}$) are also included. At $d=20 \mu\text{m}$, the average lifetime was shorter at a higher R6G concentration. However, $\langle\tau\rangle$ in the EG/W droplet was essentially the same with that

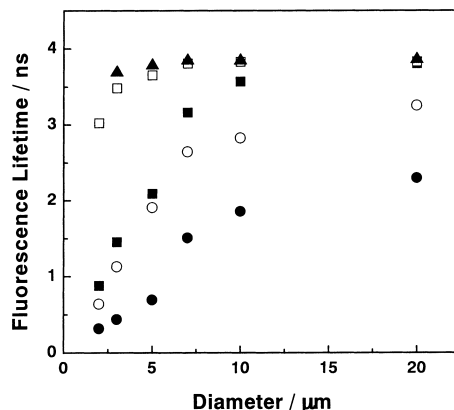


Fig. 3. Droplet size dependence of the fluorescence lifetime of R6G. $[\text{R6G}]=5 \times 10^{-3}$ (●), 2.5×10^{-3} (○), 1×10^{-3} (■), 1×10^{-4} (□), and $1 \times 10^{-5} \text{ M}$ (▲).

² Effects of fluorescence polarization on the decay curve observed under a microscope are very complicated, since incident laser pulses are focused by a large N.A. objective lens. The polarization properties of a half mirror used in this study also affect the fluorescence decay curve. In the present experimental setup, the fluorescence polarization effects could be canceled by rotating a polarizer in front of a detector system at 49.6° .

determined in the relevant bulk solution at a given [R6G]. This suggests that the [R6G] effects on $\langle\tau\rangle$ are explained by quenching of the R6G monomer emission by the dimer [35]. At $d < 20\ \mu\text{m}$, on the other hand, $\langle\tau\rangle$ decreased with a decrease in d and the size effects were much larger at a higher R6G concentration. As an example, the lifetime decreased from ~ 2 to ~ 0.3 ns on going from $d = 20$ to $2\ \mu\text{m}$ at $[\text{R6G}] = 5 \times 10^{-3}$ M. At $[\text{R6G}] < 1 \times 10^{-5}$ M, it is worth noting that the fluorescence decays single-exponentially, and the lifetime is independent of the droplet diameter. These results demonstrate clearly that the photophysics of R6G in EG/W droplets is dependent strongly on both d and [R6G].

The d and [R6G] dependencies of $\langle\tau\rangle$ resemble with those observed in EG droplets reported by Pandey and Hirayama [15]. They explained the phenomena in terms of enhanced energy transfer from an R6G monomer to a dimer with some contribution from optical-cavity effects of a microdroplet as described before. If the optical-cavity effects participate in a microdroplet, the fluorescence spectrum of a dye should exhibit size-dependent sharp structures in addition to a broad background spectrum [37,38]. In the present case, however, R6G (5×10^{-3} M) in a single microdroplet ($d = 2\ \mu\text{m}$) did not show structured fluorescence and, the shape and peak wavelength of the spectrum agreed satisfactorily with those observed in a bulk solution. Also, the fluorescence spectral band shape was independent of d ($2 \sim 20\ \mu\text{m}$). An excitation laser power dependence of the fluorescence lifetime was also not observed. Furthermore, optical-cavity effects are known to be observed only when the refractive index of a microdroplet was higher than that of the surrounding medium [39]. In the present case, the refractive index of EG/W (1.38) is smaller than that of PDMS (1.41), so that we conclude that optical-cavity effects are not the origin of the d dependence of the fluorescence lifetime of R6G in Figs. 2 and 3. Chemical processes or phenomena in individual droplets could be the primary origin of the present results. Since the reaction systems studied by us and Pandey and Hirayama are different slightly (the refractive index of EG (1.43) is slightly larger than that of a silicon oil (1.41)), we cannot compare the results directly. Nonetheless, analogous results between the two systems might suggest that chemical size-effects discussed further play a role in deciding the d dependence of the fluorescence lifetime of R6G in EG droplets dispersed in a silicon oil, other than the cavity effects.

3.2. Absorption spectroscopy of single R6G-EG/W microdroplets

In order to obtain a direct evidence of the d and [R6G] effects on $\langle\tau\rangle$, we conducted absorption spectroscopy of individual R6G (5×10^{-3} M) EG/W microdroplets³. The re-

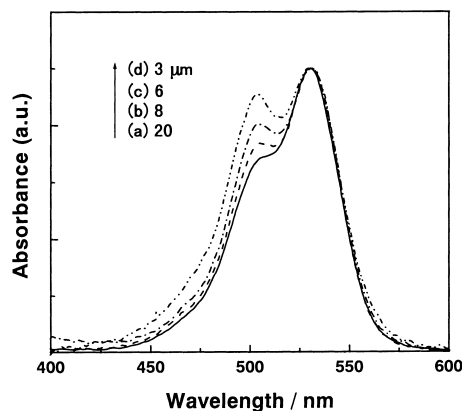


Fig. 4. Absorption spectra of R6G ($[\text{R6G}] = 5 \times 10^{-3}$ M) in single microdroplets. Droplet diameters are (a) 20; (b) 8; (c) 6; and (d) $3\ \mu\text{m}$.

sults are summarized in Fig. 4, in which the absorbance of R6G is normalized to that at the peak wavelength (around 530 nm) for comparison. The absorption spectrum for the droplet with $d = 20\ \mu\text{m}$ (a) shows the peak at around 530 nm and the shoulder around 500 nm. The spectrum determined for the microdroplet agreed very well with that in a bulk solution. Since the dye concentration is high, the bands at around 530 and 500 nm are easily assigned as the monomer and dimer of R6G, respectively [40]. When the droplet diameter is smaller than $20\ \mu\text{m}$, on the other hand, it is clear from Fig. 4 that the peak at around 500 nm increases with decrease in d . This result indicates that dimer formation of R6G in the microdroplet is facilitated with decreasing d . On the basis of these results, the droplet size dependence of $\langle\tau\rangle$ could be explained in terms of that of the dimer formation efficiency in EG/W microdroplets.

3.3. Monomer/dimer equilibrium of R6G in a bulk EG/W solution

For quantitative discussion on the d dependent dimer formation, a monomer/dimer equilibrium of R6G in a bulk solution should be known. Therefore, we conducted absorption spectroscopy on homogeneous R6G-EG/W solutions. Fig. 5 shows the absorption spectra of R6G in EG/W liquid films at various [R6G]. The absorbance ratio of the dimer to the monomer increased with increasing [R6G]. The dimer formation constant (K) can be thus determined on the basis of the results in Fig. 5. The R6G dimer formation is expressed as



and K is given by

$$K = \frac{[\text{D}]}{[\text{M}]^2} = \frac{1-x}{2Cx^2} \quad (3)$$

³ We reported earlier that the absorption spectrum of a dye in a microparticle with $d < 10\ \mu\text{m}$ was strongly affected by a probe beam size and refraction/reflection of a probe beam by the particle. In the present study, the effect of refraction/reflection of a probe beam was almost ne-

glected since the difference in the refractive index between a droplet and PDMS was very small. Furthermore, we discussed on the absorption ratio of the monomer to the dimer, so that the present discussion is not influenced largely by such experimental conditions.

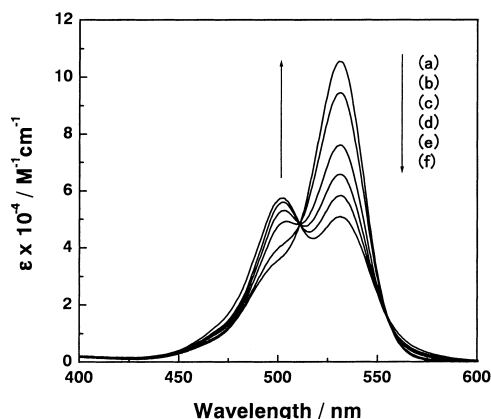


Fig. 5. Absorption spectra of bulk R6G EG/W solutions. [R6G]=(a) 1×10^{-5} ; (b) 1×10^{-3} ; (c) 5×10^{-3} ; (d) 1×10^{-2} ; (e) 2×10^{-2} ; and (f) 4×10^{-2} M.

where [M] and [D] represent the concentrations of the R6G monomer and dimer, respectively. x is the mole fraction of the monomer at a given concentration C . At a certain wavelength, both monomer and dimer absorb, so that an observed molar extinction coefficient (ε) is expressed as

$$\varepsilon = \varepsilon_{m\lambda}x + \varepsilon_{d\lambda}(1 - x) \quad (4)$$

where $\varepsilon_{m\lambda}$ and $\varepsilon_{d\lambda}$ are ε of the monomer and dimer of R6G, respectively. The $\varepsilon_{m\lambda}$ value at a given wavelength can be determined for a dilute R6G solution. The concentration-dependent spectrum in Fig. 5 was then analyzed by Eqs. (3) and (4) with ε_d and K as fitting parameters [41]. The observed data were best reproduced by the following values: $K=110 \text{ M}^{-1}$, $\varepsilon_m^{531} = 1.1 \times 10^5$, $\varepsilon_m^{502} = 3.7 \times 10^4$, $\varepsilon_d^{531} = 2.9 \times 10^4$, and $\varepsilon_d^{502} = 6.7 \times 10^4 \text{ M}^{-1} \text{ cm}^{-1}$.

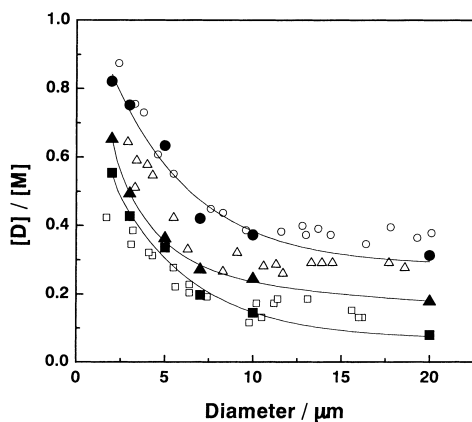


Fig. 6. Droplet size dependence of the dimer/monomer concentration ratio of R6G in single EG/W microdroplets. Open symbols; calculated from absorption spectra at the concentrations of [R6G]= 5×10^{-3} (○), 2.5×10^{-3} (△), and 1×10^{-3} M (□). Closed symbols; calculated from fluorescence lifetimes at the concentrations of [R6G]= 5×10^{-3} (●), 2.5×10^{-3} (▲), and 1×10^{-3} M (■).

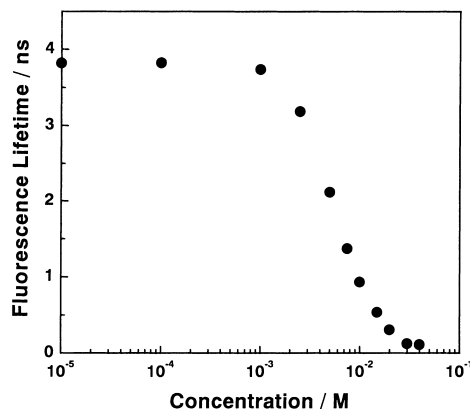


Fig. 7. Concentration dependence of the fluorescence lifetime in bulk R6G-EG/W solutions.

3.4. Droplet size-effects on R6G dimer formation

In order to reveal the origin of the d dependence of $\langle \tau \rangle$, the implication between the dimer formation efficiency and $\langle \tau \rangle$ should be clarified. First, we calculated the concentration ratio of the dimer to the monomer ($[D]/[M]$) in individual droplets on the basis of the absorption spectra of R6G in Fig. 5 and, the ε_m and ε_d values. The results are summarized in Fig. 6 as a d dependence of $[D]/[M]$ (open symbols). As seen clearly, $[D]/[M]$ increased sharply with a decrease in d . At [R6G]=5 mM, the value increased from ~ 0.4 to ~ 0.8 with a decrease in d from 10 to 2 μm . On the other hand, the $[D]/[M]$ values at $d > 10 \mu\text{m}$ were almost constant at 0.35, 0.26, and 0.13 at [R6G]=5, 2.5, and 1 mM, respectively. The $[D]/[M]$ value at a given concentration can be also calculated from Eq. (3). The calculated $[D]/[M]$ values were almost comparable to the observed value; as an example, the values were 0.33, 0.20, and 0.09 at [R6G]=5, 2.5, and 1 mM, respectively⁴. The $[D]/[M]$ ratio of R6G in a microdroplet with $d > 10 \mu\text{m}$ is essentially independent of d . This coincides very well with the absence of a d dependence of the fluorescence lifetime of R6G at $d > 10 \mu\text{m}$.

An alternate way to estimate $[D]/[M]$ is to compare $\langle \tau \rangle$ observed in an individual droplet with a concentration-dependent fluorescence decay of R6G in a bulk solution. For this purpose, we measured fluorescence lifetimes of R6G at various concentrations as shown in Fig. 7. The lifetime ($\langle \tau \rangle$) decreased significantly at [R6G]>1 mM owing to Förster-type energy transfer from the monomer to the dimer [35]. Knowing the concentration dependence of $\langle \tau \rangle$ and the K value, one can evaluate $[D]/[M]$ in single microdroplets on the basis of the observed $\langle \tau \rangle$ in the droplets and the data in Fig. 7. The $[D]/[M]$ values calculated by such procedures

⁴ At a low R6G concentration, the observed $[D]/[M]$ ratio was slightly deviated from the calculated value. This is probably due to the experimental errors in determining [D], since the absorbance change of the dimer band is very small.

are also included in Fig. 6 (closed symbols). Fig. 6 indicates that the $[D]/[M]$ values calculated from the absorption spectrum and the fluorescence lifetime agreed very well with each other at any droplet size and R6G concentration. Therefore, we concluded that the droplet size dependence of the fluorescence lifetime of R6G was ascribed to that of the dimer formation efficiency in each droplet.

3.5. Origin of the droplet size dependence of $\langle\tau\rangle$ and R6G dimer formation

The d dependence of the dimer formation could be appeared either by adsorption of R6G on the droplet/matrix interface or concentration of the droplet solution.

Adsorption of a dye on a solid/liquid or liquid/liquid interface is a well known phenomenon. In particular, dye adsorption on a droplet/solution interface is facilitated in a smaller water droplet, since the surface area/volume ratio of a droplet increases with decreasing d . Indeed, it has been reported that dimer formation of Malachite Green is facilitated in a smaller water droplet dispersed in an oil through surface adsorption of the dye on the droplet/solution interface [16–17]. Therefore, the dimer formation at the interface or a heterogeneous distribution of R6G in a microdroplet is worth elucidating in detail to discuss the origin of the d dependence of $\langle\tau\rangle$.

Dye distribution characteristics in single microparticles can be studied on the basis of a d dependence of dye absorbance as reported previously [22]. If a dye distributes homogeneously in a single particle, d corresponds to the optical path length for absorption measurements, while this is not the case for an inhomogeneous dye distribution in a particle. When a dye adsorbs on a thin surface layer of a particle, a theoretical consideration predicts that observed absorbance becomes one-third of that at a homogeneous dye distribution [22]. In the present case, however, absorbance of R6G in individual EG/W droplets agreed very well with that predicted from the molar absorptivity of the dye determined in a bulk solution. This indicates a homogeneous distribution of the dye in each EG/W droplet.

Further direct information about a dye distribution in a droplet can be obtained by using confocal fluorescence microspectroscopy with three-dimensional spatial resolution. We measured therefore fluorescence decays of R6G both at around the center of a droplet and near the droplet/PDMS interface ($d=5\text{ }\mu\text{m}$). Although the data are not shown here, the two decay profiles showed analogous results. It is worth noting that the spatial resolution (z -axis; along the excitation beam axis) of the spectroscopy system is $1\text{ }\mu\text{m}$, so that the results do not necessarily imply the absence of surface adsorption of R6G. Nonetheless, if the dimer formation at the interface is the major factor determining $\langle\tau\rangle$, the decay profile should be more or less dependent on the observation position in the droplet. Therefore, the dimer formation of R6G proceeds in the whole of an EG/W microdroplet. Both absorption and confocal fluorescence microspectroscopies

demonstrate that adsorption of R6G on the droplet/PDMS interface is not the reason for the d dependence of $\langle\tau\rangle$.

One might expect changes in the physical properties of the solvents themselves (EG and/or W). Although such an effect could be very important in submicrometer/nanometer regions, the present size-dependent dimer formation in micrometer dimension can not be explained by such the context. Vaporization of the solvent molecules should be also considered, because the samples are prepared by heating to 65°C to obtain solid PDMS/droplet films and this might lead to concentration of R6G–EG/W droplet solutions. Vaporization of ethylene glycol is not likely under the present conditions, since the boiling point of EG is 197°C . Vaporization of water will make the droplet medium less polar. If this is the case, the dimer formation of R6G in the droplet should be suppressed since that is favored in a polar medium [42]. Clearly, this is opposite to what is observed in this study.

On the other hand, permeation of EG and/or W molecules to a PDMS film might be the reason for the present results, since this also renders concentration of an R6G droplet solution. In practice, PDMS has been used as a permselective membrane for gases and liquids owing to its large three-dimensional network structures, as demonstrated for removal of aroma compounds from waste-water [43]. It has been reported that, permeability of water to PDMS is very inefficient [44], so that such an effect is neglected. If permeation of EG to the film occurs, the droplet medium becomes more polar and this should render the increase in the dimer formation efficiency. In order to test such a possibility, we measured an aging time dependence of the fluorescence decay of R6G in the droplet: just after preparation (i.e., solidification) and after several hours. However, these two measurements gave almost analogous d dependence of $\langle\tau\rangle$. The results indicate that permeation of ethylene glycol into PDMS is much slower than our measurements time scale. EG/W droplets are considered to be very stable after solidification of PDMS and, therefore, concentration of R6G in each droplet could be originated before solidification of PDMS.

Distribution of solvent molecules (EG and/or W) to PDMS before solidification will be the most probable reason for concentration of R6G in each droplet and, therefore, for the d dependence of $\langle\tau\rangle$. Distribution of EG and/or W to PDMS proceeds by diffusion of the molecules across the droplet/matrix interface. In oil-in-water or water-in-oil emulsions, mass transfer across the droplet/solution interface becomes more efficient with decreasing d owing to an increase in the surface area/volume ratio of the droplet. In the present case, droplet-to-PDMS solvent distribution before solidification of PDMS should proceed more efficiently for smaller-sized droplets, so that this brings about a higher R6G concentration in a smaller-sized droplet. The ratio of the estimated R6G concentration in an individual droplet to that for the relevant mother solution is summarized in Fig. 8. The ratio increased sharply with decreasing d at $d<10\text{ }\mu\text{m}$ and, as an example, the concentration of R6G in the droplet

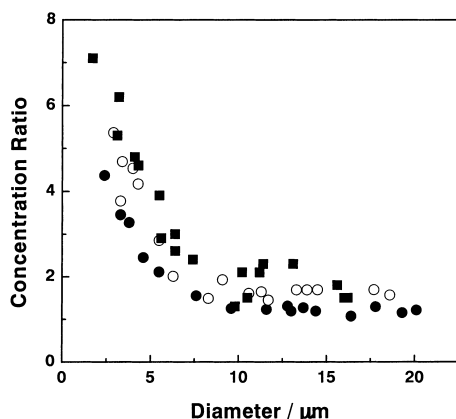


Fig. 8. Droplet size dependence of the ratio of [R6G] in a single EG/W microdroplet to that in the relevant mother solution. [R6G] = 5×10^{-3} (●), 2.5×10^{-3} (○), and 1×10^{-3} M (■).

with $d=2 \mu\text{m}$ was 5–7 times higher than the initial value (i.e., mother solution). As seen in Fig. 8, analogous behaviors were observed irrespective of the R6G concentrations.

The size-dependent [R6G] in single droplets is supposed to be preserved in the PDMS film, because PDMS before solidification is a very viscous liquid and this prevents collision of droplets. Furthermore, these non-equilibrium conditions are frozen by solidification of PDMS. The droplet size dependence of $\langle\tau\rangle$ could therefore be explained by the size dependent distribution of the solvent molecules to the PDMS film.

4. Conclusions

A dynamic fluorescence spectroscopic study revealed that the fluorescence lifetime of R6G ($\langle\tau\rangle$) in EG/W microdroplets dispersed in a PDMS matrix showed the large droplet size dependence. The fluorescence lifetime of R6G in the microdroplet decreased with the decrease in d and the increase in [R6G]. Absorption spectroscopy on individual microdroplets demonstrated that dimer formation of R6G was facilitated for smaller-sized droplets. Thus, the observed size and concentration effects on $\langle\tau\rangle$ were well explained in terms of the size-dependent dimer formation of R6G in the droplet. The smaller is a microdroplet, the larger is the surface area/volume ratio of the droplet, so that this renders that distribution of the solvent molecules to PDMS makes more efficient for smaller-sized droplet; the R6G concentration becomes higher for smaller droplets. The d dependence of $\langle\tau\rangle$ is thus appeared through more efficient R6G dimer formation in smaller-sized droplets. The size dependent fluorescence dynamics of a dye molecule in microdroplets has been reported by several research groups and discussed in terms of spherical cavity effects. As demonstrated in the present paper, however, the size dependent fluorescence dynamics also appears by the chemical effects, other than the physical effects (i.e., optical cav-

ity effects). Although further systematic investigations are needed to reveal spectroscopic and excited state properties of a molecule in micrometer-sized droplets, we suppose that both chemical and physical characteristics of a microdroplet should be considered as the possible origin of droplet size dependent phenomena. The works along the line mentioned earlier are now in progress in this laboratory.

Acknowledgements

H.B.K acknowledges to a Grant-in-Aid from the Ministry of Education, Science, Sports and Culture, Japan (No. 10440218) for the partial support of the research. The work is also supported partly by a Grant for the Priority Research Area B on 'Laser Chemistry of Single Nanometer Organic Particles' to N.K. (No. 10207201).

References

- [1] H. Masuhara, F.C. DeSchryver, N. Kitamura, N. Tamai (Eds.), *Microchemistry, Spectroscopy and Chemistry in Small Domains*, North-Holland, Amsterdam, 1994.
- [2] G. Chen, M.M. Mazumder, R.K. Chang, J.C. Swindal, W.P. Acker, *Prog. Energy Combust. Sci.* 22 (1996) 163.
- [3] H.-M. Tzeng, K.F. Wall, M.B. Long, R.K. Chang, *Opt. Lett.* 9 (1984) 499.
- [4] A. Biswas, H. Latifi, R.L. Armstrong, R.G. Pinnick, *Opt. Lett.* 14 (1989) 214.
- [5] R.L. Armstrong, J.-G. Xie, T.E. Ruekgauer, J. Gu, R.G. Pinnick, *Opt. Lett.* 18 (1993) 119.
- [6] H. Taniguchi, H. Tomisawa, *Opt. Lett.* 19 (1994) 1852.
- [7] M.M. Mazumder, G. Chen, P.J. Kindlmann, R.K. Chang, *Opt. Lett.* 20 (1995) 1668.
- [8] J. Popp, M.H. Fields, R.K. Chang, *Opt. Lett.* 22 (1997) 139.
- [9] H.-B. Lin, J.D. Eversole, C.D. Merritt, A.J. Campillo, *Phys. Rev. A* 45 (1992) 6756.
- [10] M.D. Barnes, W.B. Whitten, S. Arnold, J.M. Ramsey, *J. Chem. Phys.* 97 (1992) 7842.
- [11] M.D. Barnes, C.-Y. Kung, W.B. Whitten, J.M. Ramsey, S. Arnold, S. Holler, *Phys. Rev. Lett.* 76 (1996) 3931.
- [12] L.M. Folan, S. Arnold, S.D. Druger, *Chem. Phys. Lett.* 118 (1985) 322.
- [13] P.T. Leung, K. Young, *J. Chem. Phys.* 89 (1988) 2894.
- [14] M.D. Barnes, W.B. Whitten, J.M. Ramsey, *Chem. Phys. Lett.* 227 (1994) 628.
- [15] K.K. Pandey, S. Hirayama, *J. Photochem. Photobiol. A; Chem.* 99 (1996) 165.
- [16] H. Yao, Y. Inoue, H. Ikeda, K. Nakatani, H.-B. Kim, N. Kitamura, *J. Phys. Chem.* 100 (1996) 1494.
- [17] H. Yao, H. Ikeda, N. Kitamura, *Langmuir* 13 (1997) 1996.
- [18] N. Kitamura, K. Nakatani, H.-B. Kim, *Pure Appl. Chem.* 67 (1995) 79.
- [19] K. Chikama, K. Nakatani, N. Kitamura, *Bull. Chem. Soc. Jap.* 71 (1998) 1065.
- [20] K. Nakatani, M. Sudo, N. Kitamura, *J. Phys. Chem. B* 102 (1998) 2908.
- [21] H.-B. Kim, S. Yoshida, A. Miura, N. Kitamura, *Chem. Lett.* (1996) 923.
- [22] H.-B. Kim, S. Yoshida, N. Kitamura, *Anal. Chem.* 70 (1998) 51.
- [23] H.-B. Kim, S. Yoshida, A. Miura, N. Kitamura, *Anal. Chem.* 70 (1998) 111.

- [24] N. Kitamura, M. Hayashi, H.-B. Kim, K. Nakatani, *Anal. Sci.* 12 (1996) 49.
- [25] H.-B. Kim, M. Hayashi, K. Nakatani, N. Kitamura, K. Sasaki, J. Hotta, H. Masuhara, *Anal. Chem.* 68 (1996) 409. (correction: 68 (1996) 1987).
- [26] T. Gensch, J. Hofkens, J. van Stam, Herman. Faes, S. Creutz, K. Tsuda, R. Jerome, H. Masuhara, F.C. DeSchryver, *J. Phys. Chem. B* 102 (1998) 8440.
- [27] S. Arnold, L.M. Folan, *Rev. Sci. Instrum.* 57 (1986) 2250.
- [28] P.J. Santangelo, D. Flowers, I.M. Kennedy, *Appl. Opt.* 37 (1998) 5573.
- [29] D.A. Hinckley, P.G. Seybold, D.P. Borris, *Spectrochim. Acta A* 42 (1986) 747.
- [30] F.L. Arbeloa, T.L. Arbeloa, E.G. Lage, I.L. Arbeloa, F.C. DeSchryver, *J. Photochem. Photobiol. A; Chem.* 56 (1991) 313.
- [31] H.-B. Kim, S. Habuchi, N. Kitamura, *Anal. Chem.* 71 (1999) 842.
- [32] H.-B. Kim, S. Habuchi, M. Hayashi, N. Kitamura, *Anal. Chem.* 70 (1998) 105.
- [33] E. Grabowaska, J. Tyrzyk, C. Bojarski, *Acta Phys. Pol. A* 57 (1980) 753.
- [34] D.R. Lutz, K.A. Nelson, C.R. Gochanour, M.D. Fayer, *Chem. Phys.* 58 (1981) 325.
- [35] A. Penzkofer, Y. Lu, *Chem. Phys.* 103 (1986) 399.
- [36] C. Bojarski, R. Bujko, P. Bojarski, *Acta Phys. Pol. A* 79 (1991) 471.
- [37] A.J. Campillo, J.D. Eversole, H.-B. Lin, *Phys. Rev. Lett.* 67 (1991) 437.
- [38] P.B. Bisht, K. Fukuda, S. Hirayama, *J. Chem. Phys.* 105 (1996) 9349.
- [39] H. Fujiwara, K. Sasaki, H. Masuhara, *J. Appl. Phys.* 85 (1999) 2052.
- [40] F.L. Arbeloa, I.L. Gonzalez, P.R. Ojeda, I.L. Arbeloa, *J. Chem. Soc. Faraday Trans. 2* (78) (1982) 989.
- [41] J.E. Selwyn, J.I. Steinfeld, *J. Phys. Chem.* 76 (1972) 762.
- [42] A. Penzkofer, W. Leupacher, *J. Lumin.* 37 (1987) 61.
- [43] I.F.J. Vankelecom, S. De Beukelaer, J.-B. Uytterhoeven, *J. Phys. Chem.* 101 (1997) 5186.
- [44] T. Miyata, S. Obata, T. Uragami, *Macromolecules* 32 (1999) 3712.